Adaptive Neural Network Control of a Fully Actuated Marine Surface Vessel with Multiple Output Constraints

Zhen Zhao, Wei He, and Shuzhi Sam Ge

***Abstract*— In this brief, we investigate the control problem of tracking a desired trajectory for a fully actuated marine surface vessel considering multiple outputs constraints. To prevent multiple output constraints violation, a symmetric barrier Lyapunov function (SBLF) is employed. Backstepping, in combination with adaptive feedback approximation techniques, is introduced to design an adaptive neural network control. Experimental simulations are provided to evaluate the feasibility and effectiveness of the proposed controller. Compared to the adaptive neural network control without multiple output constraints, the proposed adaptive neural network using the SBLF can guarantee that all the outputs remain bounded.**

***Index Terms*— Adaptive neural network (NN) control, barrier Lyapunov function, marine surface vessel, multiple output constraints, trajectory tracking.**

I. Introduction

MARINE surface vessels have been widely used in many ocean engineering areas, such as oil and gas development, ocean exploration, etc., [1]–[3]. With the development of ocean engineering techniques, controlling marine surface vessels to track a predefined trajectory or follow a prescribed path has attracted more and more attention [4]–[6].

However, ensuring the stability of a marine surface vessel in harsh ocean environment is a challenging problem for nonlinear control design and development. First, vessels are always unstable without close-loop control, especially during wandering processes while withstanding storm waves. Second, the vessel dynamics are highly nonlinear and contain unknown parametric or functional uncertainties and external disturbances [7]–[9], which make the well-developed model-based control methods unfeasible. Third, the vessel dynamics always contain multiple degrees of freedom (DoFs) and are strongly coupled, such that disturbances along one DoF can easily propagate to other DoFs and further cause performance degradation or even destabilization. In addition, output constraint is also a challenge in the trajectory tracking of a marine surface vessel. Constraints generally exist in most physical systems with various forms, such as physical stoppages, saturation, as well as performance and safety specifications [10]–[13]. Violation of these constraints during operation may lead to severe performance degradation, huge economic and personnel loss, environmental pollution, etc. Therefore, it is of importance to handle these problems in the control design process for marine surface vessels.

For the first three problems, many control methods have been developed for marine surface vessels to follow desired trajectories. For example, sliding-mode tracking control methods were proposed based on explicit models [14], [15]. In recent years, adaptive neural network control schemes, in which neural networks (NNs) are primarily used as online approximators for the unknown nonlinearities due to their inherent approximation capabilities, have been found to be particularly useful for the control of nonlinear uncertain systems with unknown nonlinear functions [16]–[18]. With the help of NN approximation, it is not necessary to spend much effort on system modeling in case such modeling processes are always highly difficult and time consuming. Therefore, in this brief we utilize the NN technique to solve the first three problems in the control design process for a marine surface vessel.

For the output constraint problem in trajectory tracking for marine surface vessels, there have been relatively few works in the literature. Most of the existing approaches to tackle the constraint problem are artificial potential field (APF) [19], [20], moving-horizon optimal control [21]–[23], model-predictive control [4], [24], reference governor (RG) [25], [26], the use of set invariance [27]–[29], the barrier Lyapunov function (BLF) [10], [11], etc., which have been proven to be effective to deal with tracking problems under input/output/state constraints. The APF method defines appropriate attractive and repulsive APFs to generate dynamic constrained motion with observed state information. In the moving-horizon optimal control and model-predictive control methods, the current control action is determined by solving an online finite-horizon open-loop optimal control problem [22], which is effective for linear systems. Model-predictive control was addressed for marine surface vessels with rudder and roll constraints [4],

Manuscript received October 10, 2012; revised July 5, 2013; accepted August 27, 2013. Manuscript received in final form September 6, 2013. Date of publication October 30, 2013; date of current version June 16, 2014. This work was supported in part by the Civil Aviation University of China Research Enabling Foundation under Grant 2012QD22X, in part by the Fund of National Engineering and Research Center for Commercial Aircraft Manufacturing under Project SAMC13-JS-15- 016, in part by the Joint Funds of and in part by the National Natural Science Foundation of China and Civil Aviation Administration of China Key Project under Grant U1233201, in part by the Key Project of Tianjin Key Technology Research and Development Program under Grant 11ZCKFGX04000, in part by the Fundamental Research Funds for The Central Universities under Grant ZXH2012B002 and Grant 3122013P005, and in part by the National Natural Science Foundation of China under Grant 61203057 and the Fundamental Research Funds for the China Central Universities of UESTC under Grant ZYGX2012J087. Recommended by Associate Editor A. Alessandri.

Z. Zhao is with the College of Aerospace Automation, Civil Aviation University of China, Tianjin 300300, China (e-mail: zhenzhao0523@gmail.com).

W. He is with the Robotics Institute and School of Automation Engineering, University of Electronic Science and Technology of China, Chengdu 611731, China (e-mail: hewei.ac@gmail.com).

S. S. Ge is with the Robotics Institute and School of Computer Science and Technology, University of Electronic Science and Technology of China, Chengdu 611731, China, and also with the Department of Electrical and Computer Engineering, National University of Singapore, 117576 Singapore (e-mail: samge@nus.edu.sg).

Color versions of one or more of the figures in this paper are available online at http://ieeexplore.ieee.org.

Digital Object Identifier 10.1109/TCST.2013.2281211

where only the input and one output constraint with an explicit model were considered. The reference governor, a nonlinear device added to the primal compensated nonlinear system, was proposed to enforce the fulfillment of the constraints [30]. Since the constraints can be satisfied for the control process if and only if the initial state is contained inside an invariant set, set invariance theory plays a fundamental role in the control design process for constrained systems [29]. Compared to these methods, the BLF method is able to handle the system input/output/state constraints by virtue of a Lyapunov-based control design methodology, which avoids the need for explicit system solutions [11].

Considering that there exist parametric and functional uncertainties in the marine surface vessel dynamics, the BLF method is employed to tackle the multiple output constraints in this brief. To deal with tracking problems, this brief proposes an adaptive neural network control method for a 3-DoF actuated marine surface vessel dynamics. In the proposed method, we first tackle the problem of multiple output constraints by employing a symmetric barrier Lyapunov function (SBLF) while achieving satisfactory trajectory tracking performance. Then, nonlinearity and parametric or functional uncertainties are also considered in the control design process by using adaptive NNs to approximate the nonlinear and unknown dynamics in the system model.

The rest of the brief is organized as follows. Section II introduces the problem formulation and preliminaries. Section III elucidates the control design on a fully actuated marine surface vessel based on SBLF to deal with the multiple output constraints, and further take into account parametric or functional uncertainty in the systems. A numerical example is given in Section IV. Finally, conclusion is provided in Section V.

II. Problem Formulation and Preliminaries

The following are the notations and definitions used throughout this brief: $\mathbb{R}^n$ denotes the n-dimensional Euclidean space, $\mathbb{R}^+$ represents a positive real number, and $\|\cdot\|$ is the Euclidean vector norm in $\mathbb{R}^n$.

A. Problem Formulation

Consider the following multiple-input-multiple-output (MIMO) low-frequency motion of a 3-DoF marine surface vessel in the presence of disturbance [17]:

$$\begin{aligned} \dot{\boldsymbol{\eta}} &= J(\boldsymbol{\eta})\boldsymbol{v} \\ M\dot{\boldsymbol{v}} + C(\boldsymbol{v})\boldsymbol{v} + D(\boldsymbol{v})\boldsymbol{v} + g(\boldsymbol{\eta}) &= \boldsymbol{\tau} + d(\boldsymbol{\eta}, \boldsymbol{v}, t) \end{aligned} \tag{1}$$

where the output $\boldsymbol{\eta} = [\eta_x, \eta_y, \eta_\psi]^T \in \mathbb{R}^3$ represents the earth-frame positions and heading, respectively; $\boldsymbol{v} = [v_x, v_y, v_\psi]^T \in \mathbb{R}^3$ denotes the surge, sway, and yaw velocities in the vessel-frame coordinate system, respectively; $\boldsymbol{\tau} \in \mathbb{R}^3$ is the control input vector; $M, C(\boldsymbol{v})$, and $D(\boldsymbol{v})$, which are all unknown, represent the inertia matrix, the matrix of Coriolis and centripetal terms, and the damping matrix, respectively; $g(\boldsymbol{\eta})$ is an unknown vector of restoring forces due to ocean currents, buoyancy, and gravitational forces and moments; $d(\boldsymbol{\eta}, \boldsymbol{v}, t) \in \mathbb{R}^3$ is the unknown disturbance from the environment and/or unmodeled dynamics, among others; and $J(\boldsymbol{\eta})$ is the rotation matrix [31] defined as

$$J(\boldsymbol{\eta}) = \begin{bmatrix} \cos\eta_\psi & -\sin\eta_\psi & 0 \\ \sin\eta_\psi & \cos\eta_\psi & 0 \\ 0 & 0 & 1 \end{bmatrix}.$$

The control objective is to track a desired trajectory $\boldsymbol{\eta}_d(t) = [\eta_{xd}(t), \eta_{yd}(t), \eta_{\psi d}(t)]^T \in \Omega_{\eta d}$ while ensuring that all signals are bounded and that the outputs constraints are not violated, i.e., $\forall t \geq 0, |\boldsymbol{\eta}| \leq \boldsymbol{N}_{b_1}$.

Assumption 1: In the control design process, $\boldsymbol{v}$ and $\boldsymbol{\eta}$ are both without high-frequency parts which are caused by first-order wave-induced forces and moments.

Under Assumption 1, there is no need to do wave filtering to eliminate the high-frequency parts in $\boldsymbol{v}$ and $\boldsymbol{\eta}$ during the control design process.

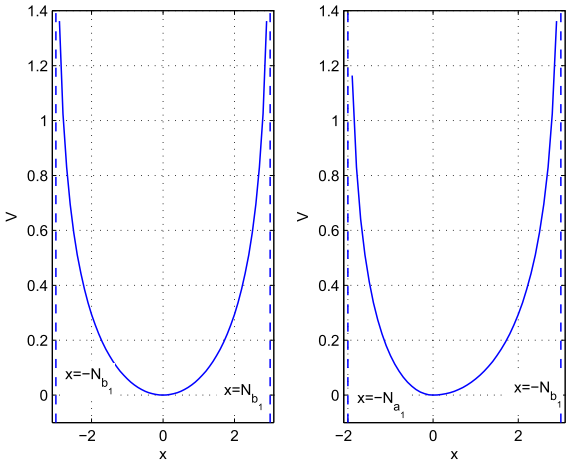

Fig. 1. Two typical Barrier Lyapunov lunctions, (left) symmetric and (right) asymmetric.

B. Preliminaries

1) Barrier Lyapunov Function

Definition 1 [32]: A BLF is a scalar function $V(x)$ defined with respect to the system $\dot{x} = f(x)$ on an open region $\mathcal{D}$ containing the origin, which is continuous and positive definite, has continuous first-order partial derivatives at every point of $\mathcal{D}$, has the property $V(x) \to \infty$ as x approaches the boundary of $\mathcal{D}$, and satisfies $V(x(t)) \leq b, \forall t \geq 0$ along the solutions of $\dot{x} = f(x)$ and some positive constant b.

For ease of display, suppose that x is a 1-D variable. A BLF may show two typical types, i.e., symmetric or asymmetric, expressed as (2) and (3), respectively. Fig. 1 illustrates the corresponding SBLF and asymmetric BLF (ABLF).

$$V_{\text{SBLF}} = \log \frac{N_{b_1}^2}{N_{b_1}^2 - x^2} \tag{2}$$

$$V_{\text{ABLF}} = \frac{q(x)}{2p} \log \frac{N_{b_1}^2}{N_{b_1}^2 - x^2} + \frac{1 - q(x)}{2p} \log \frac{N_{a_1}^2}{N_{a_1}^2 - x^2} \tag{3}$$

where p is a positive integer; $x = -N_{a_1}$ and $x = N_{b_1}$ ($N_{a_1} \neq N_{b_1}$, $N_{a_1} > 0$ and $N_{b_1} > 0$) are the left and right boundary lines for the ABLF, respectively; the SBLF is a specific form

of the ABLF, and if $N_{a_1} = N_{b_1}$, an ABLF changes to an SBLF; and

$$q(x) = \begin{cases} 1, \text{ if } x > 0 \\ 0, \text{ if } x \leq 0. \end{cases}$$

2) Neural Networks

In the literature on adaptive control, NNs are mostly used as approximation models for the unknown nonlinearities due to their inherent approximation capabilities [33], [34]. In this brief, a class of linearly parameterized NNs with radial basis functions (RBFs) is used to approximate a continuous function $f_j(Z)$: $\mathbb{R}^q \to \mathbb{R}$

$$f_j(Z) \approx W_j^T S_j(Z) \tag{4}$$

where $Z = [Z_1, Z_2, \ldots, Z_q]^T \in \Omega_Z \subset \mathbb{R}^q$ is the input vector; $W_j \in \mathbb{R}^l$ ($l > 1$ is the node number) is the weight vector; and $S_j(Z) = [s_1, s_2, \ldots, s_l]^T \in \mathbb{R}^l$. A typical choice for $S_j(Z)$ is (5)

$$S_j(Z) = \exp\left[\frac{-(Z - \mu(k))^T (Z - \mu(k))}{\sigma_k^2}\right] \tag{5}$$

where $k = 1, 2, \ldots, l$; $\mu(k) = [\mu_{k1}, \mu_{k2}, \ldots, \mu_{kq}]^T$ is the center and σ_k is the width of the neural cell of the hidden layer [35].

Universal approximation results indicate that, if l is chosen large enough, a class of linearly parameterized NNs can smoothly approximate any continuous function to any arbitrary accuracy as

$$f_j(Z) = W_j^{*T} S_j(Z) + \varepsilon^*(Z) \quad \forall Z \in \Omega_Z \tag{6}$$

where $\varepsilon^*(Z) \leq \overline{\varepsilon}$ ($\overline{\varepsilon} > 0$ is an unknown constant) is the approximation error; W_j^* is the ideal constant input vector; and $\|W_j^*\| \leq \omega_{jm}$ and defined as

$$W_j^* = \arg \min_{W_j \in \mathbb{R}^l} \left\{ \sup_{Z \in \Omega_Z} \left| f_j(Z) - W_j^T S_j(Z) \right| \right\}. \tag{7}$$

III. Control Design With an SBLF

In this brief, an approximation-based adaptive backstepping controller is employed for the 3-D marine surface vessel dynamics as (1). By incorporating a BLF in the adaptive backstepping design, the multiple output constraints are not violated at any time, including the transient phases of adaptation. By incorporating an SBLF, we employ the backstepping design as follows.

Step 1: Denote $z_1 := \boldsymbol{\eta} - \boldsymbol{\eta}_d$ and $z_2 := \boldsymbol{v} - \boldsymbol{\alpha}_1$, where $\boldsymbol{\alpha}_1$ is a stabilizing function to be designed. Choose an SBLF candidate as

$$V_1 = \sum_{i=1}^{3} \frac{1}{2} \log \frac{\boldsymbol{N}_{b_1}(i)^2}{\boldsymbol{N}_{b_1}(i)^2 - \boldsymbol{z}_1(i)^2} \tag{8}$$

where $\log(\cdot)$ denotes the natural logarithm of $\cdot$; $\boldsymbol{N}_{b_1} = \boldsymbol{N}_{c_1} - \boldsymbol{A}_0$ is the constraint of z_1, i.e., $|z_1| < \boldsymbol{N}_{b_1}$; $\boldsymbol{N}_{b_1}(i)$ and $z_1(i)$ are the ith element of $\boldsymbol{N}_{b_1}$ and z_1, respectively.

Considering that $\boldsymbol{N}_{b_1}(1) = [1\ 0\ 0]\boldsymbol{N}_{b_1}$, $\boldsymbol{N}_{b_1}(2) = [0\ 1\ 0]\boldsymbol{N}_{b_1}$, $\boldsymbol{N}_{b_1}(3) = [0\ 0\ 1]\boldsymbol{N}_{b_1}$, $z_1(1) = [1\ 0\ 0]z_1$, $z_1(2) = [0\ 1\ 0]z_1$, and $z_1(3) = [0\ 0\ 1]z_1$, V_1 can be rewritten as

$$\begin{aligned} V_1 = &\frac{1}{2} \log \frac{\boldsymbol{N}_{b_1}^T I_x \boldsymbol{N}_{b_1}}{\boldsymbol{N}_{b_1}^T I_x \boldsymbol{N}_{b_1} - z_1^T I_x z_1} \\ &+ \frac{1}{2} \log \frac{\boldsymbol{N}_{b_1}^T I_y \boldsymbol{N}_{b_1}}{\boldsymbol{N}_{b_1}^T I_y \boldsymbol{N}_{b_1} - z_1^T I_y z_1} \\ &+ \frac{1}{2} \log \frac{\boldsymbol{N}_{b_1}^T I_\psi \boldsymbol{N}_{b_1}}{\boldsymbol{N}_{b_1}^T I_\psi \boldsymbol{N}_{b_1} - z_1^T I_\psi z_1} \end{aligned} \tag{9}$$

where

$$I_x = \begin{pmatrix} 1 & 0 & 0 \\ 0 & 0 & 0 \\ 0 & 0 & 0 \end{pmatrix}$$

$$I_y = \begin{pmatrix} 0 & 0 & 0 \\ 0 & 1 & 0 \\ 0 & 0 & 0 \end{pmatrix}$$

$$I_\psi = \begin{pmatrix} 0 & 0 & 0 \\ 0 & 0 & 0 \\ 0 & 0 & 1 \end{pmatrix}.$$

For $-\boldsymbol{N}_{b_1} < z_1 < \boldsymbol{N}_{b_1}$, the SBLF candidate (9) is positive definite and C^1 continuous. Thus, it is a valid Lyapunov function candidate. The time derivative of V_1 is given by

$$\begin{aligned} \dot{V}_1 = &\frac{z_1^T I_x \dot{z}_1}{\boldsymbol{N}_{b_1}^T I_x \boldsymbol{N}_{b_1} - z_1^T I_x z_1} \\ &+ \frac{z_1^T I_y \dot{z}_1}{\boldsymbol{N}_{b_1}^T I_y \boldsymbol{N}_{b_1} - z_1^T I_y z_1} \\ &+ \frac{z_1^T I_\psi \dot{z}_1}{\boldsymbol{N}_{b_1}^T I_\psi \boldsymbol{N}_{b_1} - z_1^T I_\psi z_1}. \end{aligned} \tag{10}$$

Differentiating z_1 with respect to time yields

$$\dot{z}_1 = J(\boldsymbol{\eta})(z_2 + \boldsymbol{\alpha}_1) - \dot{\boldsymbol{\eta}}_d. \tag{11}$$

Noting that $JJ^T = I$, we choose the stabilizing function as

$$\boldsymbol{\alpha}_1 = J^T(\boldsymbol{\eta})\left[- \left(\boldsymbol{N}_{b_1}^T \boldsymbol{N}_{b_1} - z_1^T z_1\right) K_1 z_1 + \dot{\boldsymbol{\eta}}_d \right] \tag{12}$$

where $K_1 = K_1^T > 0$ is a 3×3 matrix.

Substituting (11) and (12) into (10), we have

$$\begin{aligned} \dot{V}_1 = &-3 z_1^T K_1 z_1 + \frac{z_1^T I_x J(\boldsymbol{\eta}) z_2}{\boldsymbol{N}_{b_1}^T I_x \boldsymbol{N}_{b_1} - z_1^T I_x z_1} \\ &+ \frac{z_1^T I_y J(\boldsymbol{\eta}) z_2}{\boldsymbol{N}_{b_1}^T I_y \boldsymbol{N}_{b_1} - z_1^T I_y z_1} + \frac{z_1^T I_\psi J(\boldsymbol{\eta}) z_2}{\boldsymbol{N}_{b_1}^T I_\psi \boldsymbol{N}_{b_1} - z_1^T I_\psi z_1} \end{aligned} \tag{13}$$

in which the first term on the right-hand side (RHS) is stabilizing, and the coupling term $z_1^T I_x J(\boldsymbol{\eta}) z_2 / \boldsymbol{N}_{b_1}^T I_x \boldsymbol{N}_{b_1} - z_1^T I_x z_1 + z_1^T I_y J(\boldsymbol{\eta}) z_2 / \boldsymbol{N}_{b_1}^T I_y \boldsymbol{N}_{b_1} - z_1^T I_y z_1 + z_1^T I_\psi J(\boldsymbol{\eta}) z_2 / \boldsymbol{N}_{b_1}^T I_\psi \boldsymbol{N}_{b_1} - z_1^T I_\psi z_1$ will be cancelled in the subsequent step.

Step 2: Since $\boldsymbol{v}$ does not need to be constrained, a Lyapunov function candidate by augmenting V_1 with a quadratic function is chosen as follows:

$$V_2 = V_1 + \frac{1}{2} z_2^T M z_2. \tag{14}$$

The time derivative of V_2 is given by

$$\dot{V}_2 = -3z_1^T K_1 z_1 + \frac{z_1^T I_x J(\eta) z_2}{N_{b_1}^T I_x N_{b_1} - z_1^T I_x z_1} + \frac{z_1^T I_y J(\eta) z_2}{N_{b_1}^T I_y N_{b_1} - z_1^T I_y z_1} + \frac{z_1^T I_\psi J(\eta) z_2}{N_{b_1}^T I_\psi N_{b_1} - z_1^T I_\psi z_1} + z_2^T M \dot{z}_2.$$

Differentiating z_2 with respect to time yields

$$\dot{z}_2 = \dot{v} - \dot{\alpha}_1. \tag{15}$$

Combining (15) and (1), we have

$$M\dot{z}_2 = -C(v)v - D(v)v - g(\eta) + \tau + d(\eta, v, t) - M\dot{\alpha}_1. \tag{16}$$

Substituting (16) into (15), we have

$$\dot{V}_2 = -3z_1^T K_1 z_1 + \frac{z_1^T I_x J(\eta) z_2}{N_{b_1}^T I_x N_{b_1} - z_1^T I_x z_1} + \frac{z_1^T I_y J(\eta) z_2}{N_{b_1}^T I_y N_{b_1} - z_1^T I_y z_1} + \frac{z_1^T I_\psi J(\eta) z_2}{N_{b_1}^T I_\psi N_{b_1} - z_1^T I_\psi z_1} + z_2^T \big[- C(v)v - D(v)v - g(\eta) + \tau + d(\eta, v, t) - M\dot{\alpha}_1 \big]. \tag{17}$$

Consider the following desired control law:

$$\tau = C(v)v + D(v)v + g(\eta) - d(\eta, v, t) + M\dot{\alpha}_1 - K_2 z_2 - \frac{I_x J^T(\eta) z_1}{N_{b_1}^T I_x N_{b_1} - z_1^T I_x z_1} - \frac{I_y J^T(\eta) z_1}{N_{b_1}^T I_y N_{b_1} - z_1^T I_y z_1} - \frac{I_\psi J^T(\eta) z_1}{N_{b_1}^T I_\psi N_{b_1} - z_1^T I_\psi z_1} \tag{18}$$

where $K_2 = K_2^T > 0$ is a 3×3 matrix.

Substituting (18) into (17), the latter can be rewritten as

$$\dot{V}_2 = -z_1^T K_1 z_1 - z_2^T K_2 z_2. \tag{19}$$

However, the desired control law (18) is not feasible because the process parameters $M, C(v), D(v)$, $g(\eta)$, and $d(\eta, v, t)$ are all unknown. As described in the introduction, adaptive neural network control is used to approximate the unknown part $C(v)v + D(v)v + g(\eta) - d(\eta, v, t) + M\dot{\alpha}_1$ to get

$$\tau = -K_2 z_2 - \frac{I_x J^T(\eta) z_1}{N_{b_1}^T I_x N_{b_1} - z_1^T I_x z_1} - \frac{I_y J^T(\eta) z_1}{N_{b_1}^T I_y N_{b_1} - z_1^T I_y z_1} - \frac{I_\psi J^T(\eta) z_1}{N_{b_1}^T I_\psi N_{b_1} - z_1^T I_\psi z_1} + \hat{W}^T S(Z) - \frac{N_{b_1}^T I_x N_{b_1} (z_2^T)^\dagger z_1^T K_1 z_1}{N_{b_1}^T I_x N_{b_1} - z_1^T I_x z_1} - \frac{N_{b_1}^T I_y N_{b_1} (z_2^T)^\dagger z_1^T K_1 z_1}{N_{b_1}^T I_y N_{b_1} - z_1^T I_y z_1} - \frac{N_{b_1}^T I_\psi N_{b_1} (z_2^T)^\dagger z_1^T K_1 z_1}{N_{b_1}^T I_\psi N_{b_1} - z_1^T I_\psi z_1} \tag{20}$$

$$\dot{\hat{W}}_i = -\Gamma_i (S_i(Z) z_{2i} + \varsigma_i \hat{W}_i) \tag{21}$$

where $(\cdot)^\dagger$ is the Moorse–Penrose inverse [36] of $\cdot$, $\hat{W} := \text{blockdiag}[\hat{W}_1^T, \hat{W}_2^T, \hat{W}_3^T]$ is the weight matrix of the neural network, $Z = [\eta^T, v^T, \alpha_1^T, \dot{\alpha}_1^T]^T$ is the input vector to the neural network, $S(Z) = [S_1^T(Z), S_2^T(Z), S_3^T(Z)]^T$ are the basis functions, $\Gamma_i = \Gamma_i^T > 0\,(i = 1, 2, 3)$, $z_{2i} (i = 1, 2, 3)$ are the elements of z_2, and $\varsigma_i (i = 1, 2, 3)$ are positive constants [37], [38]. The NN $\hat{W}^T S(Z)$ approximates $W^{*T} S(Z)$

$$\hat{W}^T S(Z) = W^{*T} S(Z) + \varepsilon(Z) \approx C(v)v + D(v)v + g(\eta) + M\dot{\alpha}_1 - d(\eta, v, t). \tag{22}$$

Consider the augmented Lyapunov function candidate

$$V_2 = V_1 + \frac{1}{2} z_2^T M z_2 + \frac{1}{2} \sum_{i=1}^{3} \tilde{W}_i^T \Gamma_i^{-1} \tilde{W}_i \tag{23}$$

where $\tilde{W}_i = \hat{W}_i - W_i^*$.

Combining (20) and (22), the time derivative of V_2 is given by

$$\dot{V}_2 = -3z_1^T K_1 z_1 - z_2^T K_2 z_2 - \frac{N_{b_1}^T I_x N_{b_1} z_2^T (z_2^T)^\dagger z_1^T K_1 z_1}{N_{b_1}^T I_x N_{b_1} - z_1^T I_x z_1} - \frac{N_{b_1}^T I_y N_{b_1} z_2^T (z_2^T)^\dagger z_1^T K_1 z_1}{N_{b_1}^T I_y N_{b_1} - z_1^T I_y z_1} - \frac{N_{b_1}^T I_\psi N_{b_1} z_2^T (z_2^T)^\dagger z_1^T K_1 z_1}{N_{b_1}^T I_\psi N_{b_1} - z_1^T I_\psi z_1} - z_2^T \varepsilon(z) - \sum_{i=1}^{3} \sigma_i \tilde{W}_i^T \hat{W}_i. \tag{24}$$

According to the definition of the Moore–Penrose pseudo inverse, we have

$$z_2^T (z_2^T)^\dagger = \begin{cases} 0, & \text{if } z_2 = [0, 0, 0]^T \\ 1, & \text{Otherwise.} \end{cases} \tag{25}$$

Then, we have

$$-z_1^T K_1 z_1 - \frac{N_{b_1}^T I_x N_{b_1} z_2^T (z_2^T)^\dagger z_1^T K_1 z_1}{N_{b_1}^T I_x N_{b_1} - z_1^T I_x z_1} \le -\frac{\lambda_{\min}(K_1) \Big[(N_{b_1}^T I_x N_{b_1} - z_1^T I_x z_1) + N_{b_1}^T I_x N_{b_1} z_2^T (z_2^T)^\dagger \Big] z_1^T z_1}{N_{b_1}^T I_x N_{b_1} - z_1^T I_x z_1} \tag{26}$$

where $\lambda_{\min}(\cdot)$ denotes the largest eigenvalue of the matrix $\cdot$, and $\lambda_{\min}(K_1) > 0$ for that $K_1 = K_1^T > 0$. For $|z_1| < N_{b_1}$, the following inequalities hold:

$$(N_{b_1}^T I_x N_{b_1} - z_1^T I_x z_1) + N_{b_1}^T I_x N_{b_1} z_2^T (z_2^T)^\dagger \ge N_{b_1}^T I_x N_{b_1} \tag{27}$$

$$z_1^T z_1 \ge z_1^T I_x z_1. \tag{28}$$

Therefore

$$-z_1^T K_1 z_1 - \frac{N_{b_1}^T I_x N_{b_1} z_2^T (z_2^T)^\dagger z_1^T K_1 z_1}{N_{b_1}^T I_x N_{b_1} - z_1^T I_x z_1} \le -\frac{\lambda_{\min}(K_1) N_{b_1}^T I_x N_{b_1} z_1^T I_x z_1}{N_{b_1}^T I_x N_{b_1} - z_1^T I_x z_1}. \tag{29}$$

Similarly

$$\begin{aligned}-z_1^T K_1 z_1 &- \frac{N_{b_1}^T I_y N_{b_1} z_2^T \left(z_2^T\right)^{\dagger} z_1^T K_1 z_1}{N_{b_1}^T I_y N_{b_1} - z_1^T I_y z_1} \\ &\le -\frac{\lambda_{\min}(K_1) N_{b_1}^T I_y N_{b_1} z_1^T I_y z_1}{N_{b_1}^T I_y N_{b_1} - z_1^T I_y z_1} \\ &-z_1^T K_1 z_1 - \frac{N_{b_1}^T I_\psi N_{b_1} z_2^T \left(z_2^T\right)^{\dagger} z_1^T K_1 z_1}{N_{b_1}^T I_\psi N_{b_1} - z_1^T I_\psi z_1} \\ &\le -\frac{\lambda_{\min}(K_1) N_{b_1}^T I_\psi N_{b_1} z_1^T I_\psi z_1}{N_{b_1}^T I_\psi N_{b_1} - z_1^T I_\psi z_1}. \end{aligned} \tag{30}$$

By completion of squares, we have

$$-\sigma_i \tilde{W}_i^T \hat{W}_i = -\sigma_i \tilde{W}_i^T (\tilde{W}_i + W_i^*) \le -\frac{\sigma_i}{2}\|\tilde{W}_i\|^2 + \frac{\sigma_i}{2}\|W_i^*\|^2 \tag{31}$$

and

$$-\frac{\sigma_i}{2}\|\tilde{W}_i\|^2 \le -\frac{1}{2}\sum_{i=1}^{3} \frac{\sigma_i}{\lambda_{\max}(\Gamma_i^{-1})} \tilde{W}_i^T \Gamma_i^{-1} \tilde{W}_i. \tag{32}$$

According to Young's inequality, we can obtain

$$-z_2^T \boldsymbol{\varepsilon}(Z) \le |z_2^T||\boldsymbol{\varepsilon}(Z)| \le \frac{\|z_2\|^2}{2d_1} + \frac{d_1\|\bar{\boldsymbol{\varepsilon}}\|^2}{2} \tag{33}$$

where $d_1 > 0$.

Lemma 3.1: For any positive constant column vector $\boldsymbol{b}$, the following inequality holds for any column vector $\boldsymbol{x}$ in the interval $|\boldsymbol{x}| < \boldsymbol{b}$.

$$\log \frac{\boldsymbol{b}^T \boldsymbol{b}}{\boldsymbol{b}^T \boldsymbol{b} - \boldsymbol{x}^T \boldsymbol{x}} \le \frac{\boldsymbol{x}^T \boldsymbol{x}}{\boldsymbol{b}^T \boldsymbol{b} - \boldsymbol{x}^T \boldsymbol{x}}.$$

Combining Lemma 3.1 and (26), (27), (31), (32), and (33), (24) becomes

$$\begin{aligned}\dot{V}_2 \le &-\lambda_{\min}(K_1) N_{b_1}^T I_x N_{b_1} \frac{z_1^T I_x z_1}{N_{b_1}^T I_x N_{b_1} - z_1^T I_x z_1} \\ &- \lambda_{\min}(K_1) N_{b_1}^T I_y N_{b_1} \frac{z_1^T I_y z_1}{N_{b_1}^T I_y N_{b_1} - z_1^T I_y z_1} \\ &- \lambda_{\min}(K_1) N_{b_1}^T I_\psi N_{b_1} \frac{z_1^T I_\psi z_1}{N_{b_1}^T I_\psi N_{b_1} - z_1^T I_\psi z_1} \\ &- z_2^T K_2 z_2 - \frac{1}{2}\sum_{i=1}^{3} \frac{\sigma_i}{\lambda_{\max}(\Gamma_i^{-1})} \tilde{W}_i^T \Gamma_i^{-1} \tilde{W}_i + \frac{\|z_2\|^2}{2d_1} \\ &+ \frac{d_1\|\bar{\boldsymbol{\varepsilon}}\|^2}{2} + \frac{1}{2}\sum_{i=1}^{3} \sigma_i \|W_i^*\|^2 \le -\alpha V_2 + \beta \end{aligned} \tag{34}$$

where $\alpha, \beta > 0$, and $\alpha = \min\{2\lambda_{\min}(K_1) N_{b_1}^T I_x N_{b_1}, 2\lambda_{\min}(K_1) N_{b_1}^T I_y N_{b_1}, \quad 2\lambda_{\min}(K_1) N_{b_1}^T I_\psi N_{b_1}, \}\{2\lambda_{\min}(K_2)/\lambda_{\max}(M), \sigma_i/\lambda_{\max}(\Gamma_i^{-1})(i = 1, 2, 3)\}, \beta = \|z_2\|^2/2d_1 + d_1\|\bar{\boldsymbol{\varepsilon}}\|^2/2 + 1/2\sum_{i=1}^{3} \sigma_i \omega_{im}^2$.

We are now ready to summarize our results for the state feedback case under the following theorem. Before the theorem, an assumption and two lemmas are given as follows:

Assumption 2: For any $\boldsymbol{N} > 0$, there exist positive constant 3-D vectors $\underline{\boldsymbol{Y}}_0 = [\underline{Y}_{x0}, \underline{Y}_{y0}, \underline{Y}_{\psi 0}]^T$, $\overline{\boldsymbol{Y}}_0 = [\overline{Y}_{x0}, \overline{Y}_{y0}, \overline{Y}_{\psi 0}]^T$, $\boldsymbol{A}_0 = [A_{x0}, A_{y0}, A_{\psi 0}]^T$, $\boldsymbol{Y}_1 = [Y_{x1}, Y_{y1}, Y_{\psi 1}]^T$, $\boldsymbol{Y}_2 = [Y_{x2}, Y_{y2}, Y_{\psi 2}]^T$, $\cdots$, $\boldsymbol{Y}_n = [Y_{xn}, Y_{yn}, Y_{\psi n}]^T$ satisfying $\max\{\underline{Y}_{x0}, \overline{Y}_{x0}\} \le A_{x0} < N_1$, $\max\{\underline{Y}_{y0}, \overline{Y}_{y0}\} \le A_{y0} < N_2$, and $\max\{\underline{Y}_{\psi 0}, \overline{Y}_{\psi 0}\} \le A_{\psi 0} < N_3$, such that, $\forall t \ge 0$, the desired trajectory $\boldsymbol{\eta}_d(t)$ and its several time derivatives satisfy $-\underline{Y}_{x0} \le \eta_{xd}(t) \le \overline{Y}_{x0}$, $-\underline{Y}_{y0} \le \eta_{yd}(t) \le \overline{Y}_{y0}$, $-\underline{Y}_{\psi 0} \le \eta_{\psi d}(t) \le \overline{Y}_{\psi 0}$, $|\dot{\eta}_{xd}(t)| < Y_{x1}$, $|\dot{\eta}_{yd}(t)| < Y_{y1}$, $|\dot{\eta}_{\psi d}(t)| < Y_{\psi 1}$, $|\ddot{\eta}_{xd}(t)| < Y_{x2}$, $|\ddot{\eta}_{yd}(t)| < Y_{y2}$, $|\ddot{\eta}_{\psi d}(t)| < Y_{\psi 2}, \cdots, |\eta_{xd}^{(n)}(t)| < Y_{xn}$, $|\eta_{yd}^{(n)}(t)| < Y_{yn}$, and $|\eta_{\psi d}^{(n)}(t)| < Y_{\psi n}$.

Assumption 2 implies that the desired trajectory $\boldsymbol{\eta}_d(t)$ ($\forall t \ge 0$) and its nth ($n \ge 1$) order derivatives are piecewise continuous, known, and bounded.

Lemma 3.2 [12], [32]: Let $\mathcal{Z} := \{\xi \in \mathbb{R} : -N_{a_1} < \xi < N_{b_1}\} \subset \mathbb{R}$ ($N_{a_1}, N_{b_1} \in \mathbb{R}^+$) and $\mathcal{N} := \mathbb{R}^l \times \mathcal{Z} \subset \mathbb{R}^{l+1}$ (l is a positive integer) be open sets. Consider the system

$$\dot{\varphi} = h(t, \varphi)$$

where $\varphi := [w, \xi]^T \in \mathcal{N}(w \in \mathbb{R}^l)$, and $h : \mathbb{R}^+ \times \mathcal{N} \to \mathbb{R}^{l+1}$ is piecewise continuous, and locally Lipschitz in φ, uniformly in t, on $\mathbb{R}^+ \times \mathcal{N}$. Suppose that there exist two functions $U_1 : \mathbb{R}^l \times \mathbb{R}^+ \to \mathbb{R}^+$ and $U_2 : \mathcal{Z} \to \mathbb{R}^+$, continuously differentiable and positive definite in their respective domains, such that $U_2(\xi) \to \infty$ as $-N_{a_1} < \xi < N_{b_1}$, $\gamma_1(\|w\|) \le U_1(w, t) \le \gamma_2(\|w\|)$, γ_1 and γ_2 are class K_∞ functions. Let $U(\varphi) := U_1(w, t) + U_2(\xi)$, and $\xi(0) \in \mathcal{Z}$. If the inequality

$$\dot{U} = \frac{\partial U}{\partial \varphi} h \le 0$$

holds, then $\xi(t) \in \mathcal{Z}, \forall t \in \mathbb{R}^+$.

Lemma 3.3 [16], [17], [35]: For bounded initial conditions, if there exists a C^1 continuous and positive-definite Lyapunov function $V(x)$ satisfying $\nu_1(\|x\|) \le V(x) \le \nu_2(\|x\|)$, such that $\dot{V}(x) \le -\varrho V(x) + \varsigma$, where $\nu_1, \nu_2 : \mathbb{R}^n \to \mathbb{R}$ are class K functions and $\varrho, \varsigma > 0$, then the solution $x(t)$ is uniformly bounded.

Theorem 3.2: Consider the fully actuated marine surface vessel dynamics (1) under Assumption 2, with state feedback control law (20) and adaptation law (21). For initial conditions starting in any compact set $z_1(0) \in \Omega_0 := \{z_1 \in \mathbb{R}^3 : |z_1| < \boldsymbol{N}_{b_1}\}$, the solutions of the closed-loop system are semiglobally uniformly bounded (SGUB). All closed-loop signals are bounded. And the asymptotic tracking is achieved, i.e., $\boldsymbol{\eta}(t) \to \boldsymbol{\eta}_d(t)$ as $t \to \infty$. Furthermore, the multiple output constraints are never violated, i.e., $|\boldsymbol{\eta}| < \boldsymbol{N}_{c_1}$, $\forall t > 0$.

Proof: From the previous analysis, the closed-loop stability analysis of the fully actuated marine surface vessel (1) under Assumption 2, with state feedback control law (20) and adaptation law (21) is made by Lemma III.

By solving (34), we obtain $0 \le V_2(t) \le \frac{\beta}{\alpha} + V_2(0)$, $\forall t \ge 0$. In terms of Lemma III, if $|z_1(0)| < \boldsymbol{N}_{b_1}$, we know that $|z_1(t)| < \boldsymbol{N}_{b_1}$, $\forall t > 0$. Since $\boldsymbol{\eta}(t) = z_1(t) + \boldsymbol{\eta}_d(t)$, and $\boldsymbol{\eta}_d(t) \le \boldsymbol{A}_0$ in Assumption 2, we infer that $|\boldsymbol{\eta}(t)| = |z_1(t) + \boldsymbol{\eta}_d(t)| \le |z_1(t)| + |\boldsymbol{\eta}_d(t)| < \boldsymbol{N}_{b_1} + \boldsymbol{A}_0 = \boldsymbol{N}_{c_1}$, $\forall t > 0$.

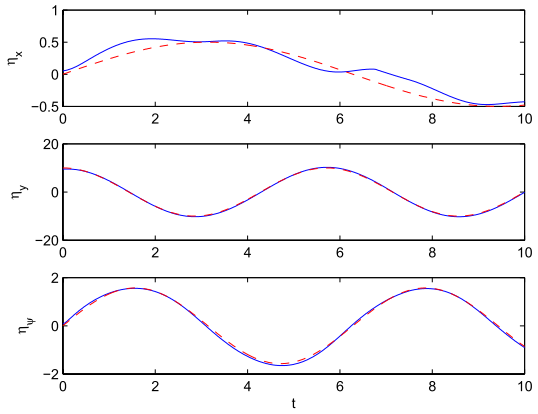

Fig. 2. Comparison between $\boldsymbol{\eta}$ (solid line) and $\boldsymbol{\eta}_d$ (dashed line).

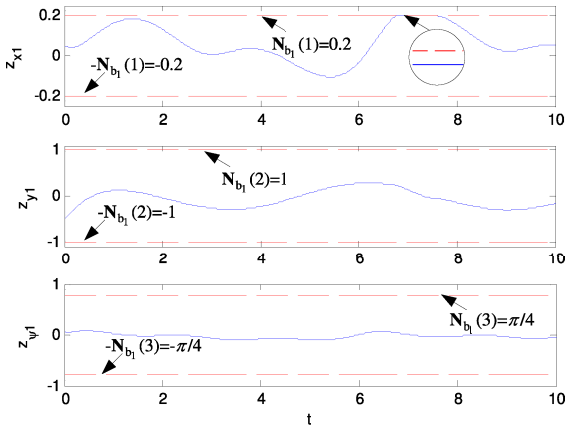

Fig. 3. Tracking error z_1 (solid line). The dashed line is the boundary.

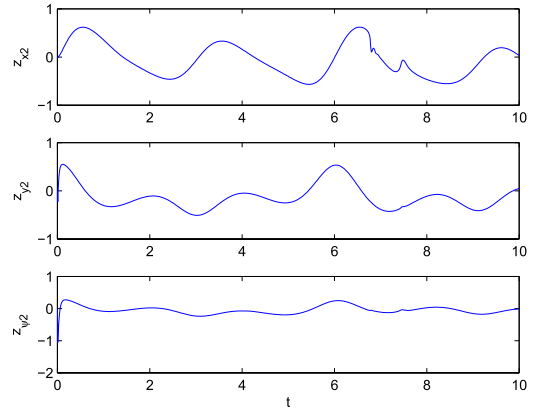

Fig. 4. Tracking error z_2.

Hence, we conclude that $\boldsymbol{\eta}$ is bounded and the multiple output constraint is never violated.

From the definition of $\boldsymbol{\alpha}_1(t)$ as (12), if $z_1(t)$ and $\boldsymbol{\eta}_d(t)$ are bounded, then $\boldsymbol{\alpha}_1(t)$ is bounded, $\forall t > 0$. Since $0 \leq V_2(t) \leq \beta/\alpha + V_2(0)$, $\forall t \geq 0$,$z_2(t)$, $\tilde{W}_i(t)$, $\hat{W}_i(t)$ and $W_i^*(t)$ are all bounded for $t > 0$. Thus, all closed-loop signals are bounded.

According to the LaSalle–Yoshizawa theorem [39], it follows that $z_1(t)$, $z_1(t) \to 0$ as $t \to \infty$. From the definition of $z_1(t)$, we deduce that $\boldsymbol{\eta}(t) - \boldsymbol{\eta}_d(t) \to 0$ as $t \to 0$. Therefore, the asymptotic tracking is achienved, i.e., $\boldsymbol{\eta}(t) \to \boldsymbol{\eta}_d(t)$, $\forall t > 0$. ■

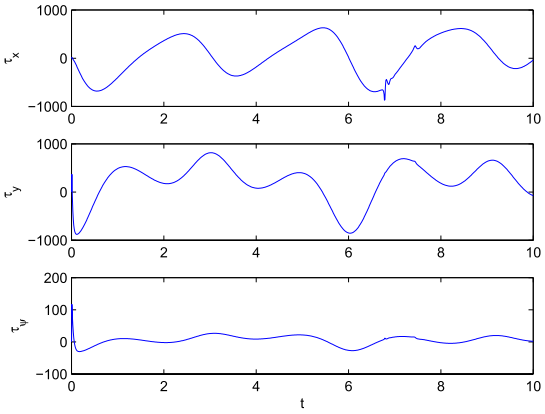

Fig. 5. Control input τ.

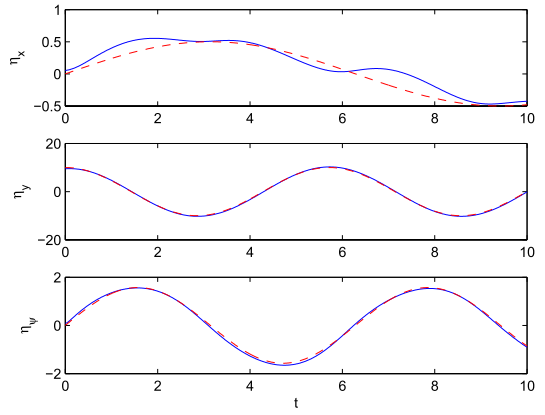

Fig. 6. Comparison between $\boldsymbol{\eta}$ and $\boldsymbol{\eta}_d$ without constraints. The dashed line is the desired trajectory, and the solid line is the real trajectory.

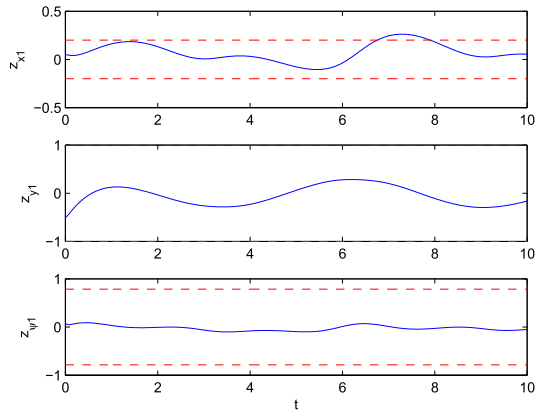

Fig. 7. Tracking error z_1 (solid line) without constraints. The dash line is the boundary.

IV. Numerical Simulations

In this section, we have considered the model of Cybership II, which is a 1 : 70 scale supply vessel replica built in a marine control laboratory in the Norwegian University of Science and Technology [17], [40].

The desired trajectories of the multiple outputs are

$$\begin{cases} \eta_{xd}(t) = 0.5 \sin 0.5t \\ \eta_{yd}(t) = 10 \cos 1.1t \\ \eta_{\psi d}(t) = \dfrac{\pi}{2} \sin t \end{cases} \tag{35}$$

subject to the multiple output constraints $|\boldsymbol{\eta}| < N_{c1} =$

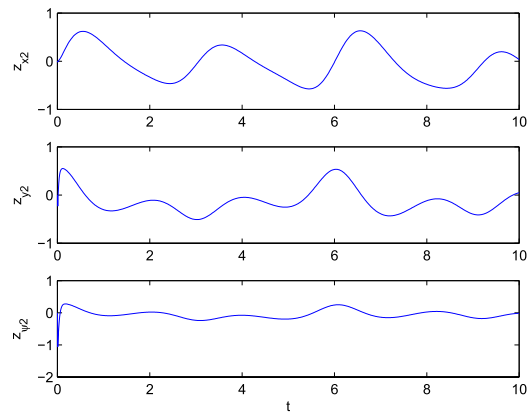

Fig. 8. Tracking error z_2 without constraints.

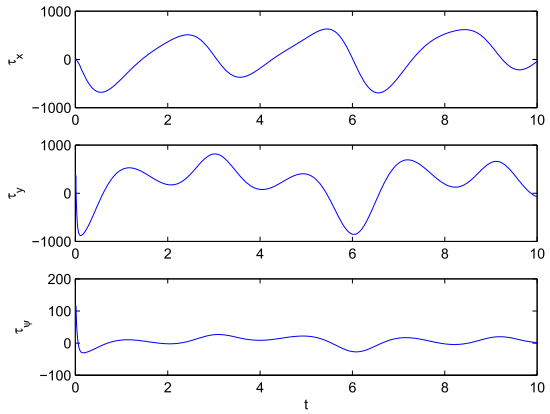

Fig. 9. Control input τ without constraints.

$[0.7, 11.0, 3\pi/4]^T$. Therefore, $N_{b1} = N_{c1} - A_0 = [0.2, 1, \pi/4]^T$, where $A_0 = [0.5, 10.0, \pi/2]^T$.

The initial conditions and the control designed parameters are chosen as follows: $\eta(0) = [0.0500, 9.5000, 0.0873]^T$; $v(0) = [0.2, 0.0, 0.0]^T$; $K_1 = \text{diag}([1, 1, 1])$; $K_2 = \text{diag}([1100, 1600, 110])$. The widths of the neural cell of the hidden layer σ_k are all 50; the initial values of the weight vectors $W_j(0)$ $(j = 1, 2, 3)$ are 50×1, 100×1, and 200×1 zero vectors, respectively. The center $\mu(k)$ in (5) are all 12×512 matrices, whose elements are 1 and -1. The updated parameters in (21) are $\Gamma_i = 0.01$, and $\varsigma_i = 0.1$ for $i = 1, 2, 3$.

The simulation results are shown in Figs. 2–5. Fig. 2 shows the comparison between the desired trajectory and the actual trajectory of the vessel. From this figure, it can be seen that the vessel tracks the desired trajectory with a high precision, and the multiple output constraints are never be violated. The tracking error z_1 is shown in Fig. 3, from which we can see that $|z_1(t)| < N_{b1}$, $\forall t > 0$. Fig. 4 shows the tracking error z_2. The control input τ is shown in Fig. 5.

Figs. 6–9 show the results without multiple output constraints. The parameters are the same as those for the former simulation. Fig. 6 is the comparison between the desired trajectory and the actual trajectory of the vessel. The tracking error z_1 without output constraints is shown in Fig. 7, from which we can see that the multiple output constraints may be violated. Fig. 8 shows the tracking error z_2 without output constraints. The control input τ without output constraints is shown in Fig. 9.

V. Conclusion

In this brief, the tracking problem for a fully actuated marine surface vessel with parametric or functional uncertainties and multiple output constraints has been investigated by using the SBLF and adaptive neural networks. It has been proven that the solutions of the closed-loop system under the proposed control are SGUB and all the closed-loop signals are bounded. Simulation results have demonstrated that the presented adaptive neural network control is feasible and effective in tracking the desired trajectory for the fully actuated marine surface vessel with multiple output constraints.

References

[1] S. S. Ge, Z. Zhao, W. He, and Y. S. Choo, "Anchor localization via magnetic induction and acoustic wireless communication network for mooring system," *IEEE J. Oceanic Eng.* [Online]. Available: http://dx.doi.org/10.1109/JOE.2013.2271957

[2] W. He, S. S. Ge, and S. Zhang, "Adaptive boundary control of a flexible marine installation system," *Automatica*, vol. 47, no. 12, pp. 2728–2734, 2011.

[3] W. He, S. S. Ge, B. V. E. How, and Y. S. Choo, *Dynamics and Control of Mechanical Systems in Offshore Engineering*. London, U.K.: Springer-Verlag, 2013.

[4] Z. Li, J. Sun, and S. Oh, "Path following for marine surface vessels with rudder and roll constraints: An MPC approach," in *Proc. Amer. Control Conf.*, Jun. 2009, pp. 3611–3613.

[5] W. He, S. S. Ge, B. V. E. How, Y. S. Choo, and K. S. Hong, "Robust adaptive boundary control of a flexible marine riser with vessel dynamics," *Automatica*, vol. 47, no. 4, pp. 722–732, 2011.

[6] S. Dai, C. Wang, and F. Luo, "Identification and learning control of ocean surface ship using neural networks," *IEEE Trans. Ind. Informat.*, vol. 8, no. 4, pp. 801–810, Nov. 2012.

[7] S. S. Ge, W. He, B. V. E. How, and Y. S. Choo, "Boundary control of a coupled nonlinear flexible marine riser," *IEEE Trans. Control Syst. Technol.*, vol. 18, no. 5, pp. 1080–1091, Sep. 2010.

[8] W. He, S. Zhang, and S. S. Ge, "Boundary control of a flexible riser with the application to marine installation," *IEEE Trans. Ind. Electron.*, vol. 60, no. 12, pp. 5802–5810, Dec. 2013.

[9] W. He, B. V. E. How, S. S. Ge, and Y. S. Choo, "Boundary control of a flexible marine riser with vessel dynamics," in *Proc. Amer. Control Conf.*, Baltimore, MD, USA, 2010, pp. 1532–1537.

[10] K. P. Tee, S. S. Ge, H. Li, and B. B. Ren, "Control of nonlinear systems with time-varying output constraints," in *Proc. IEEE Int. Conf. Control Autom.*, Dec. 2009, pp. 524–529.

[11] B. B. Ren, S. S. Ge, K. P. Tee, and T. H. Lee, "Adaptive control for parametric output feedback systems with output constraint," in *Proc. 48th IEEE Conf. Decision Control, 28th Chin. Control Conf.*, Dec. 2009, pp. 6650–6655.

[12] K. P. Tee, B. B. Ren, and S. S. Ge, "Control of nonlinear systems with time-varying output constraints," *Automatica*, vol. 47, no. 11, pp. 2511–2516, 2011.

[13] M. Chen, S. S. Ge, and B. B. Ren, "Adaptive tracking control of uncertain MIMO nonlinear systems with input constraints," *Automatica*, vol. 47, no. 3, pp. 452–465, 2011.

[14] H. Ashrafiuon and K. R. Muske, "Sliding mode tracking control of surface vessels," in *Proc. Amer. Control Conf.*, Jun. 2008, pp. 556–561.

[15] R. Yu, Q. Zhu, G. Xia, and Z. Liu, "Sliding mode tracking control of an underactuated surface vessel," *IET Control Theory Appl.*, vol. 6, no. 3, pp. 461–466, 2012.

[16] S. S. Ge and C. Wang, "Direct adaptive NN control of a class of nonlinear systems," *IEEE Trans. Neural Netw.*, vol. 13, no. 1, pp. 214–221, Jan. 2002.

[17] K. P. Tee and S. S. Ge, "Control of fully actuated ocean surface vessels using a class of feedforward approximators," *IEEE Trans. Control Syst. Technol.*, vol. 14, no. 4, pp. 750–760, Jul. 2006.

[18] B. V. E. How, S. S. Ge, and Y. S. Choo, "Control of coupled vessel, crane, cable, and payload dynamics for subsea installation operations," *IEEE Trans. Control Syst. Technol.*, vol. 19, no. 1, pp. 208–220, Jan. 2011.

[19] E. Rimon and D. E. Koditschek, "Exact robot navigation using artificial potential functions," *IEEE Trans. Robot. Autom.*, vol. 8, no. 5, pp. 501–518, Oct. 1992.

[20] J. Guldner and V. I. Utkin, "Sliding mode control for gradient tracking and robot navigation using artificial potential fields," *IEEE Trans. Robot. Autom.*, vol. 11, no. 2, pp. 247–254, Apr. 1995.

[21] D. Q. Mayne and H. Michialska, "Receding horizon control of nonlinear systems," *IEEE Trans. Autom. Control*, vol. 35, no. 7, pp. 814–824, Jul. 1990.

[22] W. B. Dunbary and R. M. Murray, "Distributed receding horizon control with application to multi-vehicle formation stabilization," *Automatica*, vol. 42, no. 4, pp. 549–558, 2006.

[23] Q. C. Nguyen and K.-S. Hong, "Transverse vibration control of axially moving membranes by regulation of axial velocity," *IEEE Trans. Control Syst. Technol.*, vol. 20, no. 4, pp. 1124–1131, Jul. 2012.

[24] D. Q. Mayne, J. B. Rawlings, C. V. Rao, and P. O. M. Scokaert, "Constrained model predictive control: Stability and optimality," *Automatica*, vol. 36, no. 6, pp. 789–814, 2000.

[25] E. Gilbert and I. Kolmanovsky, "Nonlinear tracking control in the presence of state and control constraints: A generalized referencegovernor," *Automatica*, vol. 38, no. 12, pp. 2063–2073, 2002.

[26] J. Sun and I. V. Kolmanovsky, "Load governor for fuel cell oxygen starvation protection: A robust nonlinear reference governor approach," *IEEE Trans. Control Syst. Technol.*, vol. 13, no. 6, pp. 911–920, Nov. 2005.

[27] L. Chisci, J. A. Rossiter, and G. Zappa, "Systems with persistent disturbances: Predictive control with restricted constraints," *Automatica*, vol. 37, no. 7, pp. 1019–1028, 2001.

[28] S. V. Rakovic, P. Grieder, M. Kvasnica, D. Q. Mayne, and M. Morari, "Computation of invariant sets for piecewise affine discrete time systems subject to bounded disturbances," in *Proc. 43rd IEEE Conf. Decision Control*, vol. 2. Dec. 2004. pp. 1418–1423.

[29] S. V. Rakovic, E. C. Kerrigan, K. I. Kouramas, and D. Q. Mayne, "Invariant approximations of the minimal robust positively invariant set," *IEEE Trans. Autom. Control*, vol. 50, no. 3, pp. 406–410, Mar. 2005.

[30] A. Bemporad, "Reference governor for constrained nonlinear systems," *IEEE Trans. Autom. Control*, vol. 43, no. 3, pp. 415–419, Mar. 1998.

[31] T. I. Fossen and J. P. Strand, "Nonlinear passive weather optimal positioning control (WOPC) system for ships and rigs: Experimental results," *Automatica*, vol. 37, no. 5, pp. 701–715, 2001.

[32] K. P. Tee, S. S. Ge, and E. H. Tay, "Barrier Lyapunov functions for the control of output-constrained nonlinear systems," *Automatica*, vol. 45, no. 4, pp. 918–927, 2009.

[33] S. S. Ge, C. C. Hang, T. H. Lee, and T. Zhang, *Stable Adaptive Neural Network Control*. Norwell, MA, USA: Kluwer, 2001.

[34] M. Chen, S. S. Ge, and V. B. How, "Robust adaptive neural network control for a class of uncertain MIMO nonlinear systems with input nonlinearities," *IEEE Trans. Neural Netw.*, vol. 21, no. 5, pp. 796–812, May 2010.

[35] M. Chen, S. S. Ge, and B. B. Ren, "Robust attitude control of helicopters with actuator dynamics using neural networks," *IET Control Theory Appl.*, vol. 4, no. 12, pp. 2837–2854, 2009.

[36] C. R. Rao and S. K. Mitra, *Generalized Inverse of a Matrix and its Applications*. New York, NY, USA: Wiley, 1971.

[37] W. He and S. S. Ge, "Robust adaptive boundary control of a vibrating string under unknown time-varying disturbance," *IEEE Trans. Control Syst. Technol.*, vol. 20, no. 1, pp. 48–58, Jan. 2012.

[38] W. He, S. Zhang, and S. S. Ge, "Boundary output-feedback stabilization of a Timoshenko beam using disturbance observer," *IEEE Trans. Ind. Electron.*, vol. 60, no. 11, pp. 5186–5194, Nov. 2013.

[39] M. Krstic, I. Kanellakopoulos, and P. Kokotovic, *Nonlinear and Adaptive Control Design*. New York, NY, USA: Wiley, 1995.

[40] R. Skjetne, T. I. Fossen, and P. V. Kokotovic, "Adaptive maneuvering, with experiments, for a model ship in a marine control laboratory," *Automatica*, vol. 41, no. 2, pp. 289–298, 2005.